Naval Research Laboratory
Washington, DC 20375-5320

NRL/MR/6750--96-7821

Use of an Active Wire B_θ Cell for Electron Beam Conditioning

D.P. MURPHY
M.C. MYERS
J.A. ANTONIADES
R.F. FERNSLER
R.A. MEGER

Charged Particle Physics Branch
Plasma Physics Division

D.J. WEIDMAN

Nicolet Imaging Systems
San Diego, CA

April 19, 1996

DISCLAIMER NOTICE

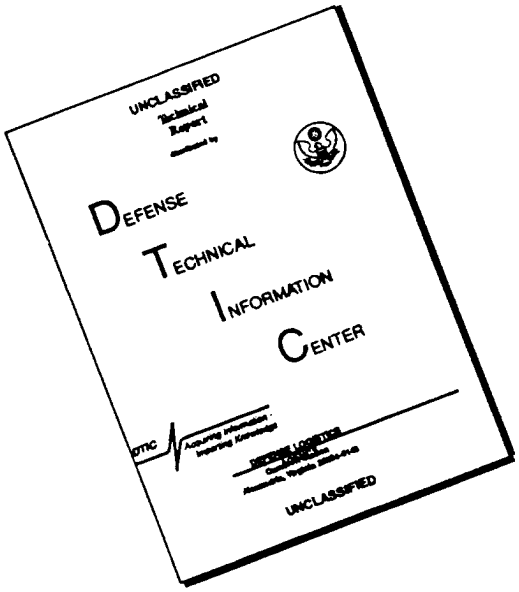

THIS DOCUMENT IS BEST QUALITY AVAILABLE. THE COPY FURNISHED TO DTIC CONTAINED A SIGNIFICANT NUMBER OF PAGES WHICH DO NOT REPRODUCE LEGIBLY.

REPORT DOCUMENTATION PAGE

Form Approved
OMB No. 0704-0188

1. AGENCY USE ONLY (*Leave Blank*)	2. REPORT DATE	3. REPORT TYPE AND DATES COVERED
	April 19, 1996	Interim

4. TITLE AND SUBTITLE

Use of an Active Wire B_θ Cell for Electron Beam Conditioning

5. FUNDING NUMBERS

PE - 61153N

6. AUTHOR(S)

D.P. Murphy, M.C. Myers, D.J. Weidman*, J. Antoniades, R. Fernsler, and R.A. Meger

7. PERFORMING ORGANIZATION NAME(S) AND ADDRESS(ES)

Naval Research Laboratory
Washington, DC 20375-5320

8. PERFORMING ORGANIZATION REPORT NUMBER

NRL/MR/6750–96-7821

9. SPONSORING/MONITORING AGENCY NAME(S) AND ADDRESS(ES)

Office of Naval Research
800 North Quincy Street
Arlington, VA 22217-5660

10. SPONSORING/MONITORING AGENCY REPORT NUMBER

11. SUPPLEMENTARY NOTES

*Nicolet Imaging Systems, San Diego, CA 92121

12a. DISTRIBUTION/AVAILABILITY STATEMENT

Approved for public release; distribution unlimited.

12b. DISTRIBUTION CODE

13. ABSTRACT (*Maximum 200 words*)

The propagation of intense, relativistic electron beams in air is subject to the resistive hose instability. Conditioning the beam prior to injecting it into the air can extend its range by reducing the hose growth rate and by reducing the initial spatial perturbations that seed the hose instability. Experiments have been performed using the SuperIBEX accelerator (I_{peak} = 10-30 kA, E = 4.5 MeV, 40 ns FWHM) and various conditioning cells to suppress hose. This paper describes the performance of an active wire B_θ cell that was used in conjunction with an IFR cell. The IFR cell detunes the instability by producing a head-to-tail radius taper on the beam. The wire cell maintains this radius taper while producing an emittance taper that is necessary to suppress the hose growth. In addition, the wire cell reduces the initial beam perturbations through the anharmonic centering force associated with the wire current and its azimuthal magnetic field B_θ. The ability of the B_θ cell to reduce the beam offset with a minimal increase in the beam radius gives it several advantages over the use of a simple, thick scattering foil to perform the radius taper to emittance taper conversion. The SuperIBEX beam propagation distance, in terms of the betatron oscillation scale length, was extended to $\sim 10\lambda_\beta$ using these cells.

14. SUBJECT TERMS

Electron beam
Conditioning
Hose instability

15. NUMBER OF PAGES

33

16. PRICE CODE

17. SECURITY CLASSIFICATION OF REPORT	18. SECURITY CLASSIFICATION OF THIS PAGE	19. SECURITY CLASSIFICATION OF ABSTRACT	20. LIMITATION OF ABSTRACT
UNCLASSIFIED	UNCLASSIFIED	UNCLASSIFIED	UL

NSN 7540-01-280-5500

Standard Form 298 (Rev. 2-89)
Prescribed by ANSI Std 239-18
298-102

CONTENTS

USE OF AN ACTIVE WIRE B_θ CELL FOR ELECTRON BEAM CONDITIONING

I. INTRODUCTION

The primary obstacle to the propagation of intense, relativistic electron beams in air over a long distance is the resistive hose instability. This instability can completely disrupt a beam after propagation distances as short as several beam diameters. Fernsler et al.[1] have shown theoretically that hose growth can be suppressed, but not eliminated, by proper preparation of the beam prior to injection into air. The resistive hose is a convective instability originating in the interaction between the beam and the background plasma. It develops as lateral beam motion which couples to the natural radial betatron oscillations of beam electrons in the beam's self fields. That is, the growth rate is determined by k/k_β, where k is the perturbation wavenumber and k_β is the beam betatron wavenumber. Once excited at a particular point in the beam, the instability will grow and couple from slice to slice back toward the tail, ultimately disrupting the beam propagation due to large amplitude beam motion. The key to minimizing the growth is to spoil the resonance between subsequent portions of the beam, while at the same time decreasing the transverse perturbations which seed the instability. Variations in k_β with time τ detune hose such that the peak component of hose growth is limited to a maximum value of $\exp(0.6/\eta)$, where[1,2]

$$\eta \equiv (1-f)\tau_d \frac{\partial}{\partial \tau} \ln\left(k_\beta\right) \tag{1}$$

is the detuning parameter. Here f is a plasma return-current fraction, and τ_d is a magnetic dipole decay time. To keep hose growth under 50 requires $\eta > 0.15$. In that case, initial beam offsets no larger than 2% of the beam radius, i.e., $\delta y_i \sim 0.02 r_b$, can be tolerated without disrupting the beam.

Manuscript approved March 18, 1996.

Theory shows that one can decrease the hose growth by changing the beam emittance as a function of time within the beam pulse. This can be accomplished by imposing an emittance taper to the beam from head to tail thereby altering the resonant frequencies so that the instability does not couple well. At the same time the amplitude of beam motion which initiates the instability can be reduced. In equilibrium, the detuning parameter can be rewritten as[2]

$$\eta \approx 0.1f - (1-f)\tau_d \frac{\partial}{\partial \tau} \ln(\varepsilon_n). \qquad (2)$$

In the beam head and body $f < 1$, and thus the normalized beam emittance ε_n must decrease with τ to keep $\eta > 0.15$. The decrease needed depends strongly on the beam current I_b, because τ_d (which measures the plasma conductance) rises at a rate proportional to I_b. Spoiling the resonance between subsequent portions of the beam is not sufficient. The transverse perturbations which seed the instability must decrease at the same time. This is usually accomplished by smearing out any coherent motion of the beam centroid at the expense of increased beam emittance. The application of beam emittance tailoring and sweep reduction is called beam conditioning. The conditioning goals for SuperIBEX are as follows: (i) reduce the beam offsets to $\delta y_i \sim 0.02 r_b$, and (ii) tailor ε_n to keep $\eta > 0.15$. The latter requires ε_n to fall by more than 3 to 1 from beam head to tail for SuperIBEX parameters.

In the SuperIBEX beam propagation experiment, beam conditioning is applied in two stages. First the beam is passed through an Ion Focused Regime (IFR) cell to produce the desired radius taper, and second, an active wire B_θ cell is used to center the beam and remove perturbations introduced by the accelerator and to convert the radius taper to emittance tailoring. Once the beam emerges into full density air, it will propagate in a self-pinched equilibrium that reflects a balance between the beam's emittance-driven pressure and its self magnetic field. The

beam emittance generated in the B_θ cell must match that required for the beam current and radius at injection into the propagation region, or else additional beam heating and radius growth will result.

The IFR cell consists of a 40 cm long hollow tube filled with ~5 mTorr argon. Beam electrons entering the IFR cell ionize the background gas, producing a low density plasma. Plasma electrons are expelled by the beam space charge leaving a neutralizing ionic space charge. The final degree of space charge neutralization is determined by the gas pressure and the beam pulse length. Initially the beam expands in the IFR cell under the influence of its emittance and negative space charge. As the space charge is neutralized, the magnetic field from the beam current pinches the beam radially. As a result, the beam reaching the end of the IFR cell shows a decreasing radius as a function of time from the beam head back into the body. This radius taper is then converted into an emittance taper by passing the beam through a scattering foil or through a following B_θ cell. Theory predicts that if the resultant emittance taper is large enough, the growth of the hose motion can be kept to a factor of 10-100 above the initial sweep or perturbation amplitude. For stable propagation the final hose amplitude should be no more than the beam radius, to keep the beam inside of the beam-generated plasma channel. Thus one needs to keep the perturbation amplitude to 0.1-0.01 times the beam radius. For low beam current operations, IFR conditioning alone can be sufficient for stable propagation for a few meters distance. However, higher beam current operations with IFR conditioning alone have proven difficult.[3] Several papers have been published detailing IFR cell operation and experimental results.[4,5,6,7,8]

Removal of beam sweep, beam centering, as well as conversion of radius tapering to emittance tapering is accomplished by the active wire B_θ cell,[9,10] first developed by C. Frost.

This must be accomplished without negating the radius taper produced by the first stage IFR cell. As designed for this experiment, the B_θ cell is an evacuated ($<10^{-5}$ Torr) metal cylinder, 20 cm diameter by 80 cm long, with a thin (0.32 mm diameter) on-axis wire tightly stretched between titanium end foils (0.04 mm thick). An external capacitor bank drives a current in the wire (hence the term active wire) in the same direction as the electron beam current. The current driven in the wire produces a magnetic field, $B_\theta \sim I_{wire}/r$, where I_{wire} is the wire current, and this field directs the beam electrons toward the wire axis. The net force on the beam electrons comes from the wire current alone, since the forces from the image current and image charge induced on the wire by the beam cancel to first order. The wire force is anharmonic, and it centers the beam through orbit phase-mixing at the cost of increased emittance. The beam thus leaves the wire cell centered about the wire, with an emittance determined by the wire current and the injected beam radius and offset.

The operation of the B_θ cell is the focus of this paper. Section II discusses design issues associated with the B_θ cell, while Section III discusses the conversion of radius tailoring to emittance tailoring. Section IV discusses matching the beam from the B_θ cell into the air. Section V details experiments performed on SuperIBEX, followed by conclusions in Section VI.

II. B_θ CELL DESIGN ISSUES:

Self pinched relativistic electron beam propagation relies on a balance between the beam's radial electrostatic and magnetic forces and the beam's transverse pressure. The electric and magnetic forces cause the electrons to oscillate round the force center. The amplitude of these oscillations depends on the perpendicular energy of the electrons while the oscillation frequency ω_β depends on the field strength. Axial motion of the electrons is close to *c*, the speed

of light, and produces a natural spatial scale length $2\pi c/\omega_\beta$ called the betatron wavelength λ_β. In an evacuated wire cell, the externally driven wire current superimposes a radially dependent, azimuthal magnetic field, $B_\theta(r) = 2I_{wire} / rc$. The magnetic force exerted on the beam electrons is then $F_{wire} = 2eI_{wire}/rc$. Such an anharmonic force makes the oscillation frequencies of the individual electrons depend on the initial radius at which an electron entered the cell. The distance along the cell axis needed for an electron to make one orbit around the central wire is its betatron wavelength, and this distance is longest for electrons which start farthest from the wire. Since the electrons, starting from different radii, take different amounts of time to orbit the wire, the electron orbits get out of phase with each other and become incoherent. This incoherence smears out transverse motion of the beam relative to the wire. Phase-mixing thus centers the beam on the wire. The beam then adopts the wire as its new center, at the expense of an increase in perpendicular energy due to orbit smearing. Figure 1 is a depiction of this process of centering an offset, unstable beam. Inside the cell, the longest betatron wavelength for the electron that starts farthest from the wire is given by:[2]

$$\lambda_\beta = 2r_{max}\sqrt{\frac{\pi I_{Alfven}}{I_{wire}}} \qquad (3)$$

where r_{max} is the maximum initial radius and I_{Alfven} is the Alfven current ($17\beta\gamma$ kA). The factor $\beta\gamma$ is ~10 since β is v/c ~1 and the usual relativistic mass factor γ is ~10 in this experiment. Equation (3) is derived in the Appendix. An average betatron wavelength $\overline{\lambda}_\beta$ can be calculated by finding the average radius for the beam . It depends on the beam radial profile but is approximately:

$$\bar{\lambda}_\beta \approx 2r_{1/2}\sqrt{\frac{\pi I_{\text{Alfven}}}{I_{\text{wire}}}} \tag{4}$$

where $r_{1/2}$ is the beam half-current radius. The length $\bar{\lambda}_\beta$ is the minimum necessary for phase-mixing to spread the beam sufficiently that it becomes centered on the wire. The limiting parameters allowed for in this SuperIBEX experiment are $r_{1/2} \leq 2.5$ cm and $I_{wire} \geq 2$ kA. This yields $\bar{\lambda}_\beta \leq 80$ cm, which was the length chosen for the B_θ cell for the SuperIBEX experiment.

At any time τ within the beam pulse, there is an initial characteristic beam radius $r_{bo}(\tau)$ and possibly a spatial offset from the beam axis $\delta y_o(\tau)$. Phase mixing and beam centering effects within the cell cause the beam radius to grow to a final value:[11]

$$r_{bf}(\tau) \approx \sqrt{r_{bo}^2(\tau) + \delta y_o^2(\tau)}. \tag{5}$$

As long as the initial offset of any slice is small, i.e., $\delta y_o(\tau) \leq r_{bo}(\tau)/2$, the ~ 3:1 head-to-tail radius taper from the IFR cell is not washed out by the wire cell.

III. BEAM HEATING WITHIN THE B_θ CELL

In addition to centering the beam, the B_θ cell serves to convert the radius tailoring from the IFR cell into the emittance tailoring needed for hose detuning. The simplest way to convert a radius taper to an emittance taper is to pass the beam through a thick scattering foil. A scattering foil converts a small amount of axial energy into perpendicular energy or beam temperature. On average, the beam electrons gain the same amount of temperature, independent of their radius. If the scattering foil is thick enough, the beam temperature introduced by the foil will be much larger than the initial beam temperature. The beam emittance which is the product of the beam

radius and the square root of its temperature, will then become a function of the radius when the beam hits the foil. Thus the radial profile will determine the emittance profile. For a foil, the beam temperature gained by the beam electrons is:[7]

$$T_{\text{foil}} = \gamma mc^2\left(\frac{d}{2\gamma^2}\right) \tag{6}$$

where d is the thickness of titanium foil in mils (.001"). For the wire cell the equivalent temperature gain of the beam electrons is related to the force exerted on the beam electrons by the wire current. The average temperature added to the beam electrons by the wire is:

$$T_{\text{wire}} = \left\langle \frac{\mathrm{r}\cdot \mathrm{F}_{\text{wire}}}{2} \right\rangle = \frac{\mathrm{e}I_{\text{wire}}}{\mathrm{c}} = \gamma mc^2\left(\frac{I_{\text{wire}}}{I_{\text{Alfven}}}\right) \tag{7}$$

where $\mathrm{F}_{\text{wire}} = eI_{wire}/rc$ is the force exerted on the beam from the wire current I_{wire} and $I_{\text{Alfven}} = 17\beta\gamma\,\text{kA} \approx 170\,\text{kA}$ for SuperIBEX parameters. A comparison of Eqs. (6) and (7) gives

$$\frac{T_{\text{foil}}}{T_{\text{wire}}} = \frac{\left(\frac{d}{2\gamma^2}\right)}{\left(\frac{I_{\text{wire}}}{I_{\text{Alfven}}}\right)} \approx \frac{d/200}{I_{\text{wire}}/170} \approx 0.85\frac{d}{I_{\text{wire}}}\,. \tag{8}$$

Thus for each 1 kA of wire current, the beam heating is about the same as that produced by 1.18 mil of titanium foil. The advantage of the B_θ cell is that it also centers the beam while it converts the radius taper into an emittance tailoring.

IV. BEAM MATCHING INTO AIR

Almost as important as beam radius tailoring and damping of radial motion is the transition of the beam from the conditioning cells to the air. If the beam parameters produced by the conditioning cells are significantly different from the equilibrium parameters in the air, the beam will have to adjust. This adjustment can dominate the beam conditioning, negating the beneficial effects. Thus one must match the output beam as closely as possible to the equilibrium propagation beam.

An electron beam propagating in air relaxes to a Bennett equilibrium with a temperature of $T_\perp = eI_{eff}/2c$, where the effective pinch current I_{eff} depends on the radial distribution of both the beam current and the plasma current induced within the beam.[12] The smaller the beam temperature $T_\perp$, the smaller the equilibrium radius. If a transverse temperature larger than $T_\perp$ is added in the conditioning cells, the beam radius in air will be determined by the heating within the conditioning cells. But if the transverse temperature is equal to or less than $T_\perp$, the beam propagates at the minimum radius achievable from the system.[13] The matching condition at the exit of the B_θ cell foil can be written at peak beam current as:

$$T_{\text{match}} = T_{\text{wire}} + T_{\text{foil}} = \frac{e}{c}\frac{I_{eff}}{2} \tag{9}$$

where I_{eff} is the maximum pinch current in the air propagation region. Experimentally one can measure the beam current I_{beam} and the net current I_{net}, which is the sum of the beam current and the total induced plasma current inside and outside the beam. The effective current I_{eff} can only be estimated from numerical simulations and is ~0.8 I_{beam} under SuperIBEX conditions.[1,14] Combining Eqs. (8) and (9) gives the matching condition:

$$T_{\text{match}} \approx T_{\text{wire}}\left(1+\frac{0.85d}{I_{\text{wire}}}\right) \tag{10}$$

where d is the thickness of the Titanium exit foil and I_{wire} is in kA. For the SuperIBEX beam propagating in air,[1] the matching condition becomes:

$$I_{eff} \approx 0.8 \cdot I_{beam} \approx 2 \cdot I_{wire}\left(1+\frac{0.85\,d}{I_{wire}}\right), \tag{11}$$

$$\text{or} \qquad I_{wire} \approx 0.4 \cdot I_{beam} - 0.85\,d. \tag{12}$$

Typically, d = 1.5 mils (.0015") and $I_{\text{beam}} \geq 15$ kA, so the matching condition in the body of the beam pulse is:

$$\frac{I_{wire}}{I_{beam}} \approx 0.3\,. \tag{13}$$

This means that the optimum wire current for matching the beam into the air is ~$0.3I_{beam}$. If the beam can be stabilized at this value of wire current, it will be properly emittance matched to its effective current in full density air as it exits the B_θ cell. If a higher wire current is used, then additional radius growth would be expected due to the mismatch between the cell and the air equilibrium.

If the emittance tailoring is instead performed by an IFR cell alone, the equation for matching the beam temperature into air is as follows:

$$T_{\text{match}} = T_{\text{foil}} = \frac{e}{c}\frac{I_{\text{effective}}}{2} = \gamma mc^2\left(\frac{d}{2\gamma^2}\right). \tag{14}$$

So for a thickness d in mils of titanium and beam current in kA:

$$d = \frac{\gamma^2 I_{eff}}{I_{Alfven}} \approx \frac{I_{beam}}{2} \text{ for SuperIBEX parameters.} \qquad (15)$$

This means that to compare the effects of an IFR only cell with an IFR/B_θ cell, one should use the appropriate matching conditions. It will require ~7.5 mils of foil to match a 15 kA SuperIBEX beam to the air using an IFR cell only, while it takes ~4.5 kA of wire current to do the same job with the B_θ cell that has a 1.5 mil thick output foil.

In air, the betatron wavelength $\bar{\lambda}_\beta$ depends the effective current in a manner similar to Eq. (4) for the betatron wavelength inside the wire cell. In air it is:[1,15]

$$\bar{\lambda}_\beta \approx 2\pi r_{1/2}\sqrt{\frac{I_{Alfven}}{I_{eff}}} \quad . \qquad (16)$$

Since for SuperIBEX, $I_{Alfven} \approx 170$ kA and $I_{eff} \approx 0.8 \cdot I_{beam}$, then $\bar{\lambda}_\beta \approx 50/\sqrt{j_{beam}}$ where $j_{beam} = I_b / \pi r_{1/2}^2$ is the current density in kA/cm^2. The beam half current radius $r_{1/2}$ is measured downstream of the conditioning cells to determine how much the beam has been heated. The measurement is taken ~ $1\bar{\lambda}_\beta$ downstream of the exit foil to allow the beam to reach its equilibrium radius and it is also used to estimate how far the beam propagates in terms of the resistive hose instability scale length.

V. EXPERIMENTAL RESULTS

A. Apparatus

The SuperIBEX accelerator uses a field emission diode to produce the 4.5 MeV, 40 ns long electron beam pulse used in these experiments.[16] Diodes of this type are susceptible to

localized emission fluctuations which can seed the beam with random transverse motion. The random movements can feed the resistive hose instability, leading to beam stability problems downstream. Conditioning of the beam after the acceleration phase is designed to reduce the intensity of these instabilities and to prepare the beam for propagation in full density air. Figure 2 shows a photograph and a sketch of the IFR and B_θ cell on SuperIBEX. The IFR cell is within the rightmost, 20 cm diameter by 40 cm long 4-way cross. The 20 cm diameter by 80 cm long B_θ cell is inside the central 4-way cross and bellows sections. The beam propagates from the SuperIBEX accelerator, to the right of the picture, through the conditioning cells to the full density air propagation region, to the left of the picture. The propagation region is inside a 2 m diameter by 5 m long instrumented chamber (see Fig. 3). Within the chamber are mounted open-shutter cameras, net current and beam current monitors and a Cerenkov light emitter. A critically damped, external capacitor circuit (58 μF, 1.55 μH, $\frac{1}{4}$ ~15 μs) drives current in the wire for the B_θ cell operation. The central wire, which carries 2-10 kA is #28 AWG tinned copper wire (0.32 mm diameter). The SuperIBEX accelerator is triggered so the electron beam enters the B_θ cell at peak wire current.

B. Transport through the B_θ cell

Figure 4 shows measurements of beam current, current density and radial profile from a Segmented Faraday Cup[17] (SFC) measured just before and just after the B_θ cell. The SFC is a radially segmented charge collector that measures the radial profile of the current distribution. Within experimental error, Shot 2116 and Shot 2063 had the same initial conditions. The data demonstrates that the radial profile and peak current density are not significantly degraded by passing the beam through the B_θ cell. In particular, the radius taper ratio of about 3:1 from the

beam head to just past the peak current is maintained. This taper in the beam radius, when converted by the B_θ cell to emittance tailoring, detunes the hose instability and decreases its growth rate.[7] A 1.5 mil thick titanium foil was used at the exit of the IFR cell. Another 1.5 mil thick titanium foil was used at the end of the B_θ cell. The wire current in Shot 2116 is 3 kA. It was observed that if there is no externally driven wire current, $I_{wire} = 0$, then the electron beam will be pushed into the wall inside the B_θ cell by an oppositely directed current induced on the wire by the beam itself. No beam emerges from the cell.

C. Comparison of IFR only and IFR/B_θ conditioning

Figure 5 shows open-shutter photographs of three high beam current (>15 kA), IFR only shots (5 mTorr argon), each with a different thickness of titanium foil at the exit of the IFR cell. No B_θ cell is used on these three shots. The effect of increasing the foil thickness from 15 to 20 and then to 25 mils increases the transverse temperature of the beam, thereby increasing the final beam radius r_b. The resistive hose growth rate scales as $\lambda_\beta^{-1} \propto r_b^{-1}$. A fatter beam may go farther but has a lower current density. The peak current density, measured 25 cm downstream of a 25 mil thick IFR exit foil, is typically down to less than 0.6 kA/cm^2. A small amount of centering occurs because the wall of the IFR cell used was only 10 cm in diameter.[4] For low current beams, wall centering seems sufficient to compensate for small initial offsets within the IFR cell. However, these high current beams suffer from greatly increased transverse motion inside the IFR cell. The field of view in the photos is 1.1 m wide, starting 2.3 m from the end of the IFR cell. The beam in the top photo (Fig. 5a) has gone unstable even before it enters the field of view. The beam in the middle photo (Fig. 5b) is beginning to go unstable at the end of the field of view. The beam is the bottom photo (Fig. 5c) has been heated so much by the 25 mil exit

foil that it became almost too diffuse to photograph. The titanium exit foil that would convert this 17 kA beam's radius taper to emittance tailoring and match the beam into air would be about 8 mils thick, which is one-third the thickness of foil actually needed to stabilize the beam for 3.4 m of propagation. For this beam the betatron wavelength is calculated to be 65 cm or more, so it has only propagated about $4\bar{\lambda}_\beta$ at the left edge of the field of view of the photo. Note that the beam does have the correct emittance tailoring, but the transverse perturbations are such that disruptive hose growth develops rapidly. Only by overheating the beam to greatly inflate its radius and thereby increase it betatron wavelength could propagation over a few meters distance be accomplished.

Figure 6 shows open-shutter photos of three shots using an IFR cell followed by a B_θ centering cell. The IFR cell here is 10 cm diameter for most of its length but expands to 20 cm diameter near its end to allow the beam head to expand. However, the larger cell diameter permits the beam to be more off-center as it enters the B_θ cell. The shot-to-shot variation of the beam offset at the entrance to the B_θ cell was measured to be as much as 100% of the beam radius. The titanium exit foil at the end of the B_θ cell is only 1.5 mils thick, so that beam heating is dominated by the wire current [see Eq. (10)]. The 15 kA beam in the top photo (Fig. 6a) passed through a B_θ cell with 3.9 kA of wire current. It is just beginning to go unstable at the end of the field of view. The beam in the middle photo (Fig. 6b) is comparable in current to the upper and lower photos and was centered by a 4.3 kA wire current, and the bottom photo (FIG. 6c) shows an 18 kA beam centered by a 6.3 kA wire current. Based on the current density of a similar beam measured just downstream of the B_θ cell, the 18 kA beam in the last photo has a

betatron wavelength of about 25 cm. The left edge of the field of view is 3.2 m downstream of the B_θ cell so the beam has propagated stably for over $10\bar{\lambda}_\beta$.

One of the diagnostics used to provide time resolved information on beam stability is a fast framing camera which images the Cherenkov light emitted when the beam passes through a thin piece of quartz or Teflon placed in the beam path.[18] Cherenkov light intensity is proportional to the local current density. This Gated Optical Imager (GOI)[19] camera takes four images[20] with a 2 ns shutter gate at user defined times within the beam pulse. Figure 7 shows an open-shutter, Polaroid photograph and four GOI frames taken as the beam passed through a quartz plate 170 cm downstream of the B_θ cell exit foil. The GOI frames give the absolute beam position and therefore can be used to estimate the amplitude of the hose oscillation. The beam offset is measured from the center of the target to the beam centroid position in the image. The beam offset is a combination of the hose oscillation and possibly a small misalignment of the B_θ cell toward the target. A GOI camera image is 704 x 528 pixels, and the field of view is adjusted so the resolution is about 12.5 pixels/cm at the target. Analysis of the images fixes the centroid position to within ±0.25 cm. The centroid position is found based on all current density values within a given contour intensity profile (0%, 10%, 20%, ..., 100%). Due to slight asymmetries in the beam shape the centroid position derived for each profile is can vary as much as ±0.25 cm from the average of the position locations. The profile of the beam can also be determined from the frame by taking lineouts through the center of the image and fitting either a Gaussian or Bennett profile to the data as shown in Fig. 8. It is sometimes difficult to determine which of the profiles is the better fit to the data. The beam should evolve to a Bennett profile as it propagates in air.

Figure 9 shows data from two series of shots using the GOI to determine the time resolved radial offset of the beam from the center of the Cherenkov target as a function of the ratio of the B_θ wire current to the beam current for similarly radius tailored beams. The chart in Fig. 9(a) shows beam offsets for a series of shots with the Cerenkov target within 25 cm of the B_θ cell exit. A linear regression line drawn through the data shows the increasing effectiveness of the active wire cell in decreasing the beam offset as the wire current ratio is increased. The chart in Fig. 9(b) presents a similar set of measurements taken with the Cerenkov target at either 170 cm or 190 cm from the end of the cell. The trend line through this data again shows the decrease in beam motion as the current ratio is increased. At low values of wire current, there is apparently insufficient damping and centering during the beam transit of the 80 cm long B_θ cell to stabilize the beam. Indeed Eqs. (3) and (4) indicate that the 80 cm long cell may be too short for the beam to come to equilibrium when the wire current is low. This leads to large amplitude beam offsets measured at the downstream target. At wire current to beam current ratios higher than ~30%, the matching condition of Eq. (13) is violated. This mismatch overheats the beam in air, thereby lowering the current density downsteam of the B_θ cell. Still the B_θ cell is more effective at stabilizing the beam than a thick exit foil IFR cell by itself. For a similarly radius tailored beam, an IFR exit foil 25 mils thick was needed to propagate a high current beam "stably" for ~3 m downstream. The same propagation distance was achieved using 6.3 kA of wire current and a 1.5 mil thick exit foil, with a factor of three decrease in the transverse temperature added to the beam during conditioning (recall that 1 kA of wire current is equivalent to ~1 mil of foil for heating). In terms of the distance scaled to the hose growth scale length λ_β,

the beam from the B_θ cell traveled several times farther than the beam from the thick exit foil, IFR cell.

Magnetic probe measurements of the net current centroid motion in the propagation chamber show the same decrease in hose motion with increasing wire to beam current ratio. Figure 10 presents data from a set of magnetic probes 60 cm downstream of the B_θ exit foil. The data points were chosen at times coincident with GOI images of the beam and are from the same data run. This position data is accurate to only ±20%, mainly due to electrical noise on the signals.

SFC measurements and GOI images of a target placed at Z<25cm from the end of the B_θ cell show the minimum beam radius is ≤1.5 cm. As seen in Fig. 9(a), even at high wire current ratios (~0.6), the measured offset is still large, ~ 10% of the beam radius. Nevertheless, the conditioning demonstrably improved stability, enabling the beam to propagate at least $10\bar{\lambda}_\beta$.

VI. CONCLUSION

An active-wire B_θ cell was demonstrated to be an effective tool for reducing the initial perturbations which feed the growth of the resistive hose instability during the propagation of intense, relativistic electron beams in air. The radius taper produced in the IFR cell was successfully converted to an emittance taper. The beam offset measured at ~25 cm (~1 λ_β) into the air decreased as the ratio of the wire current to beam current increased. At relatively high ratios (~0.6) the beam offset at injection was still ~10% of the beam radius. This may have been due to large beam offsets at injection into the B_θ cell. Nevertheless, hose stability improved markedly using the B_θ cell. This is presumably due to the damping of the beam oscillations

during the transit through the B_θ cell. The propagation distance, in terms of the betatron wavelength, improved to at least $10\bar{\lambda}_\beta$. For an IFR only case, it was necessary to significantly overheat a radius tailored beam with a thick foil to stabilize the hose instability. A thick exit foil heats the beam and lowers the current density as well as mismatching the beam into the air, producing further radius growth. Thus the beam current density can be significantly higher when an active wire cell is used.

ACKNOWLEDGMENTS

The authors would like to thank R. E. Pechacek, T. A. Peyser, S. P. Slinker, and R. F. Hubbard for their experimental and theoretical contributions to this experiment. We would also like to thank W. D. Dolinger, G. W. Littlejohn, J. P. Picciotta and A. K Noll for their technical assistance with the SuperIBEX accelerator. This work supported by the Office of Naval Research.

APPENDIX: λ_β in a B_θ Wire Cell

The magnetic field from a wire current I_{wire} produces a radial force on the beam electrons given in Gaussian units by $F_{wire} = 2e\beta I_{wire}/rc$, where βc is the axial speed of the electrons. The radial position $r(t)$ of an electron thus varies in time according to

$$\gamma m \frac{d^2 r}{dt^2} = \frac{\gamma m}{2} \frac{d}{dr}\left(\frac{dr}{dt}\right)^2 = -\frac{2e\beta I_{wire}}{rc} \quad . \tag{A1}$$

This equation can be immediately integrated to yield

$$\frac{dr}{dt} = 2\left[\frac{e\beta I_{wire}}{\gamma mc} \ln(r_{max}/r)\right]^{1/2} \quad . \tag{A2}$$

The electron reaches its minimum radius, r_{min}, after a time

$$\tau = \int_{r_{min}}^{r_{max}} dr\left(\frac{dr}{dt}\right)^{-1} = \left(\frac{\gamma mc}{4e\beta I_{wire}}\right)^{1/2} \int_{r_{min}}^{r_{max}} dr\left[\ln(r_{max}/r)\right]^{-1/2} \quad . \tag{A3}$$

In the limit that $r_{min} \to 0$, this reduces to

$$\tau \to \frac{\sqrt{\pi}}{2}\left(\frac{\gamma mc}{e\beta I_{wire}}\right)^{1/2} r_{max} \quad . \tag{A4}$$

The electron then crosses to the other side of the wire and back again, taking 4τ to completely orbit the wire. The betatron wavelength in this case is therefore given by:

$$\lambda_\beta = 4\beta\tau c = 2r_{max}\sqrt{\frac{\pi I_{Alfven}}{I_{wire}}} \quad , \tag{A5}$$

where, $I_{Alfven} = \beta\gamma mc^3/e$. Note that this value differs only by a factor of $(2/\pi)^{1/2} \cong 0.8$ from the betatron wavelength required for a circular orbit of the same maximum radius:

$$\lambda_{\beta c} = \left(\beta c / v_\theta\right) 2\pi r_{\max} = \pi r_{\max} \sqrt{\frac{2 I_{Alfven}}{I_{wire}}} \ , \tag{A6}$$

where

$$v_\theta = \sqrt{r_{\max} F_{wire} / \gamma m} = \sqrt{2 e \beta I_{wire} / \gamma m c} \tag{A7}$$

is the electron orbital velocity.

References

[1]R. F. Fernsler, S. P. Slinker, M. Lampe, and R. F. Hubbard, Physics of Plasmas, **2**, 4338, (1995).

[2]R. F. Fernsler, et al., in Proceedings of the 9th International Conference on High-Power Particle Beams, edited by D. Mosher and G. Cooperstein (Naval Research Laboratory, Washington, DC 1992), pp. 1276-1281. See NTIS Document No. PB92206168. Copies may be ordered from the National Technical Information Service, Springfield, VA 22161. The price is $175.00 plus $8.00 handling fee.

[3]W. M. Fawley, Bull. Am. Phys. Soc. **35**, 1054 (1990).

[4]J. A. Antoniades, et al., in Proceedings of the 8th IEEE Pulsed Power Conf., edited by K. Prestwich and R. White (IEEE Press, New York, NY, 1991), pp. 582-584.

[5]M. C. Myers, J. A. Antoniades, R. A. Meger, D. P. Murphy, R. F. Fernsler, and R. F. Hubbard, J. Appl. Phys. **78** (6), 3580 (1995).

[6]K. W. Struve, et al. ,in Proceedings of the 5th International Conference on High-Power Particle Beams, edited by R. J. Briggs and A. J. Toepfer (Pub. by Lawrence Livermore National Laboratory, Livermore, CA, 1983), pp. 408-411. See NTIS Document No. DE83017620. Copies may be ordered from the National Technical Information Service, Springfield, VA 22161. The price is $46.50 plus $8.00 handling fee.

[7]J. A. Antoniades, et al., in Proceedings of the 8th IEEE Pulsed Power Conf., edited by K. Prestwich and R. White (IEEE Press, New York, NY, 1991), pp. 585-588.

[8]R. F. Fernsler, R. F. Hubbard, and S. P. Slinker, Phys. Fluids B **4**, 4153 (1992).

[9]C. A. Frost, et al, in Proceedings of the 9th International Conference on High-Power Particle Beams, edited by D. Mosher and G. Cooperstein (Pub. by Naval Research Laboratory, Washington, DC 1992), pp. 109-118. See Ref. 2.

[10]D. P. Murphy, et al, in Proceedings of the 9th International Conference on High-Power Particle Beams, edited by D. Mosher and G. Cooperstein (Pub. by Naval Research Laboratory, Washington, DC 1992), pp. 1251-1256. See Ref. 2.

[11] R. F. Fernsler, et. al., in Proceedings of the 10th International Conference on High-Power Particle Beams, edited by A. Kolb, R. White and W. Rix (Pub. by Maxwell Laboratories, San Diego, Ca, 1994) p. 622. See NTIS Document No. PB95144317. Copies may be ordered from the National Technical Information Service, Springfield VA 22161. The price is $105.00 plus $8.00 handling fee.

[12]E. P. Lee, Phys. Fluids **19**, 60 (1976).

[13]Stanley Humphries, Jr., Charged Particle Beams, (John-Wiley and Sons Inc., New York, (1990), p. 582.

[14] R. F. Hubbard, M. Lampe, S. P. Slinker, and G. Joyce, Phys. Fluids **31**, 2349 (1988).

[15] D. J. Weidman, K. T. Nguyen, M. J. Rhee, R. F. Schneider, and R. A Stark, J. Appl. Phys. **76** (6) 3244 (1994).

[16] R. A. Meger, et. al., in Proceedings of the 6th IEEE Pulsed Power Conference, edited by P. J. Turchi and B. H. Bernstein (IEEE Press, New York, 1987), p502.

[17]T. A. Peyser, J. A. Antoniades, M. C. Myers, M. Lampe, R. E. Pechacek, D. P. Murphy, and R. A. Meger, Rev. Sci. Instrum. **62** (12), 2895 (1991).

[18] John Galayda, in AIP Conference Proceedings 212, Accelerator Instrumentation, edited by E. R. Beadle and V. J. Castillo (American Institute of Physics, New York 1990) pp. 59-84.

[19] P. E. Young, J. D. Hares, J. D. Kilkenny, D. W. Phillion, and E. M. Campbell , Rev. Sci. Instrum. **59** (8), 1457 (1988).

[20]D. P. Murphy, T. A. Peyser, and R. E. Pechacek, Rev. Sci. Instrum. **65** (3), 762 (1994).

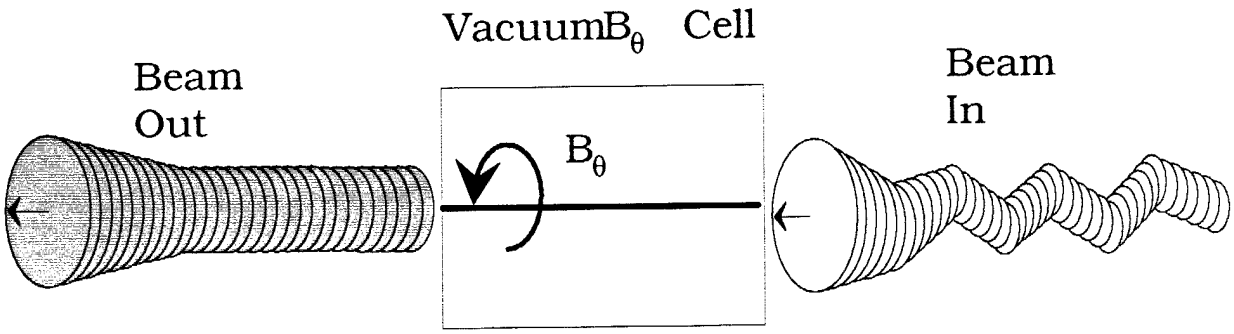

FIG. 1. A depiction of the centering process inside the B_θ cell. An off-center beam, seeded with random motion enters the cell from the right. The centering process smears out the oscillations and forces the beam to accept the wire axis as its new center.

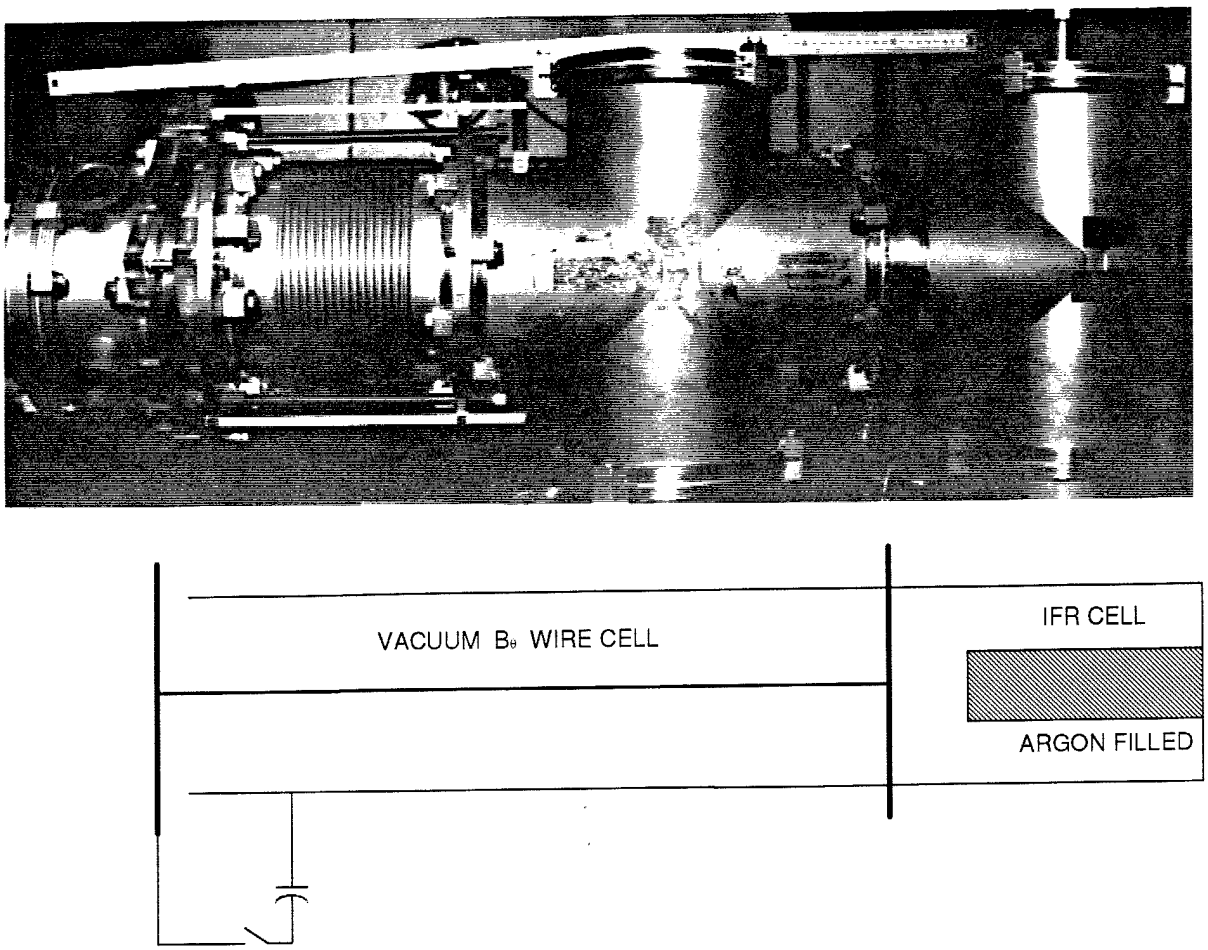

FIG. 2. A photograph (a) and a sketch (b) of the IFR cell and B_θ cell hardware. In the photo, the 20 cm diameter by 40 cm long IFR cell is inside the rightmost 4-way cross. It has a 10 cm diameter by 30 cm long metal tube inside to provide a small amount of wall centering to the beam. The head of the beam is allowed to expand to a full 20 cm diameter before the beam enters the B_θ cell. The 20 cm diameter by 80 cm long B_θ cell is inside the central 4-way cross and bellows sections. A 2.5 cm thick, insulating Lucite plate separates the exit foil holder from the main body of the B_θ cell. A meter stick is laying across the top of the B_θ cell. The SuperIBEX accelerator is out of view to the right, and the full density air propagation region is out of view to the left. The sketch shows the external capacitor bank and triggered switch which are used to drive current down the central wire in the B_θ cell.

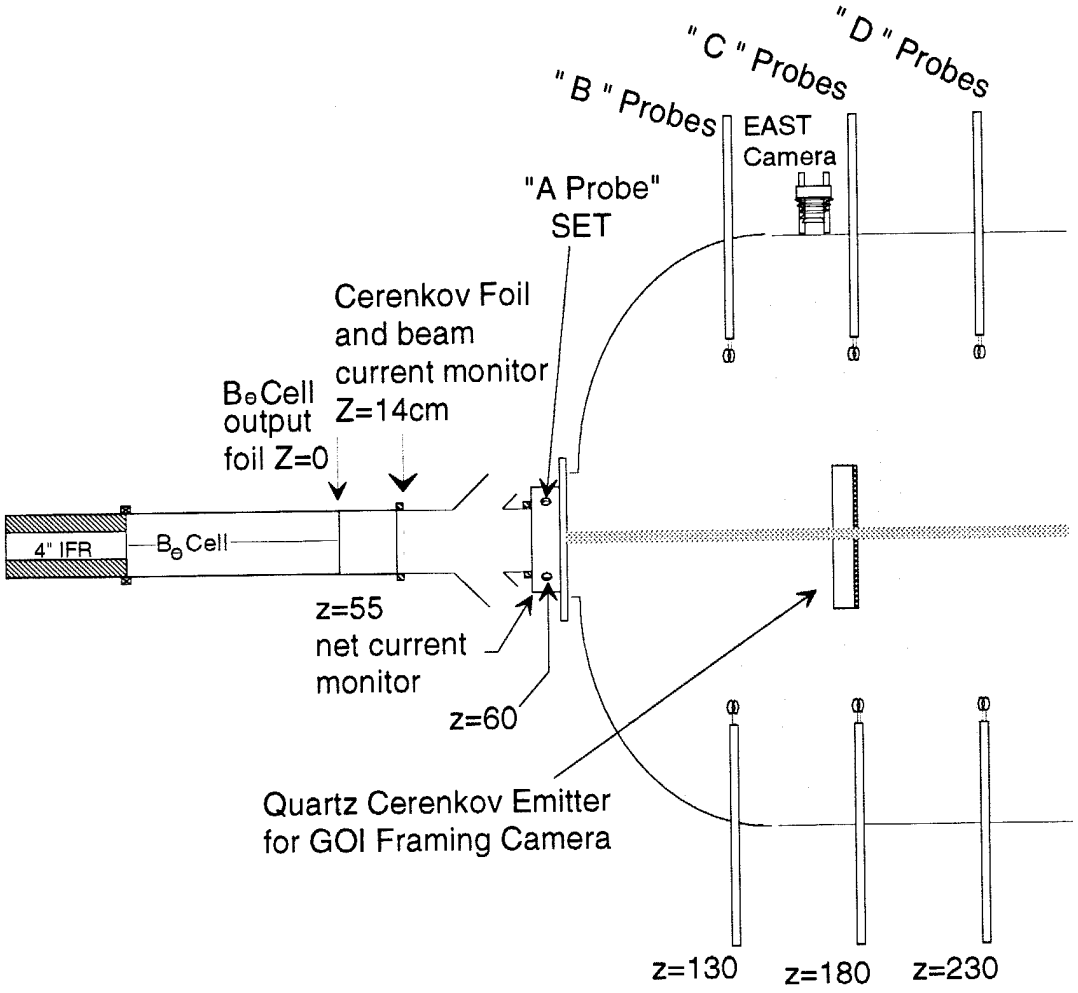

FIG. 3. A schematic drawing of the conditioning cells and the full density ai chamber. The chamber is 2 m diameter by 5 m long and has various net cur beam position and Cerenkov light optical diagnostics installed.

(a)

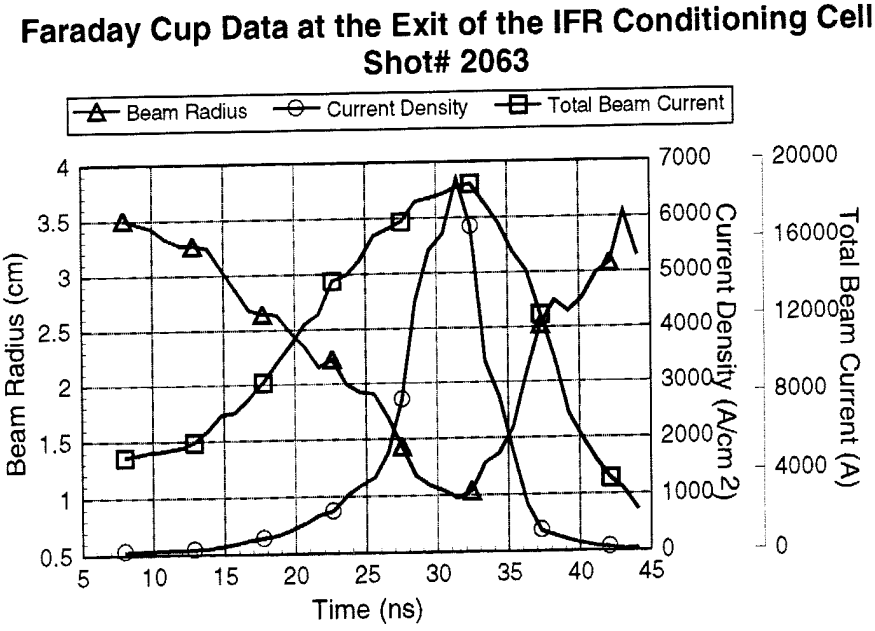

(b)

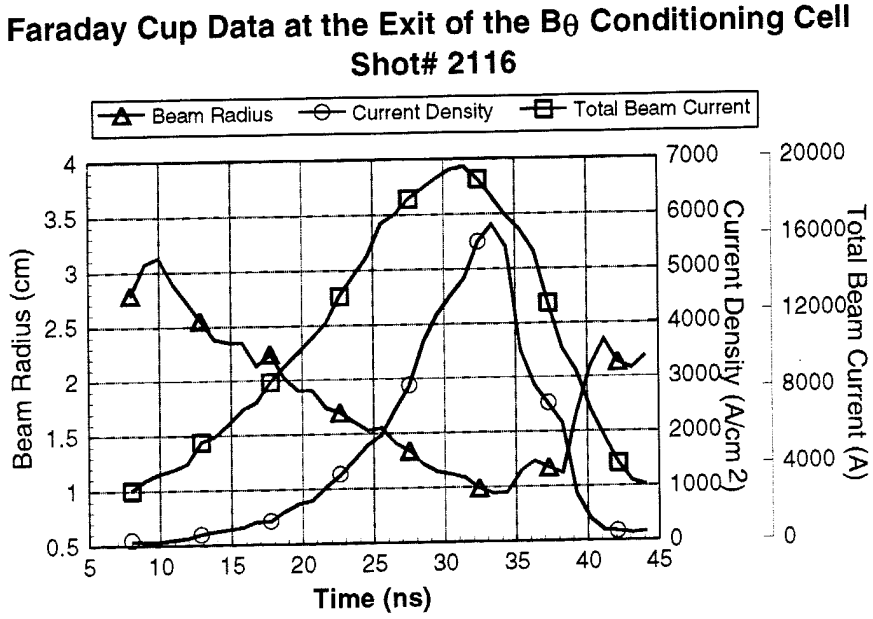

FIG. 4. The upper graph (a) shows data from a Segmented Faraday Cup mounted at the exit of the IFR cell. No B_θ cell is used. The lower graph (b) shows data from a corresponding shot with the Faraday Cup mounted at the exit of the B_θ cell which followed the IFR cell. The wire current in the second shot is 3 kA.

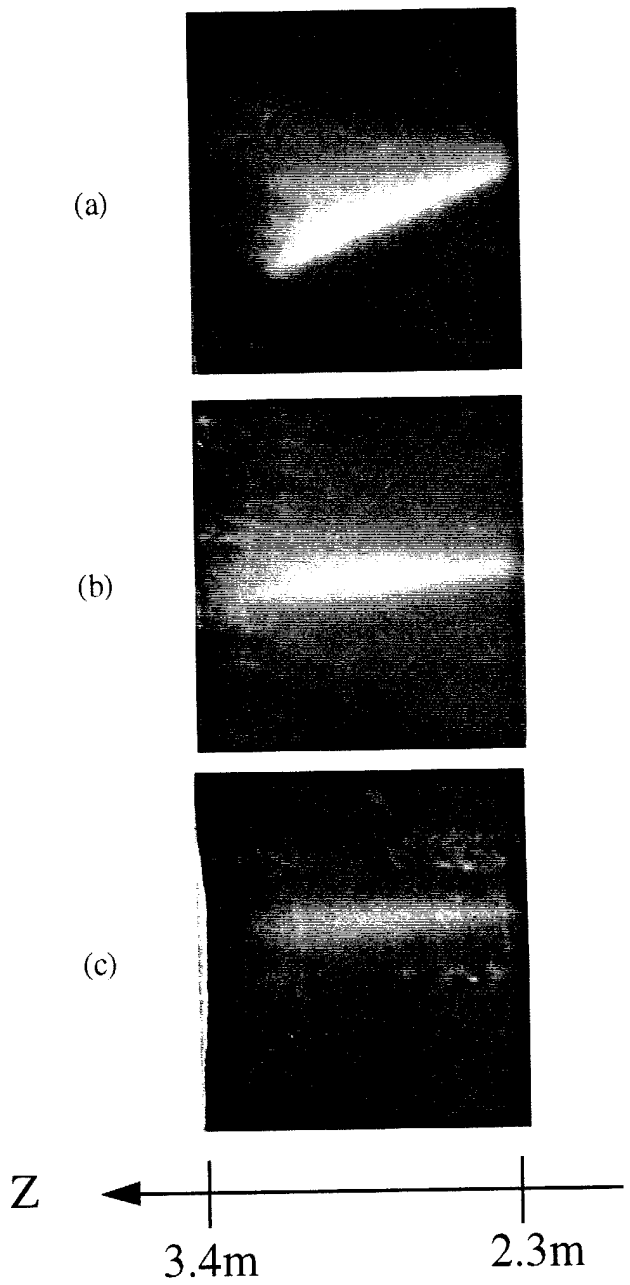

FIG. 5. Open-shutter photographs of three high current beams propagating in full density air. Conditioning is provided by an IFR cell only. Photo (a) is from shot #1041. The IFR cell is 10 cm diameter by 40 cm long. The output foil is 15 mils thick titanium. Peak beam current is 21 kA. The e-beam is propagating from right to left in full density air. The photo shows the range between 2.3 m and 3.4 m downstream of the IFR cell. Photo (b) is from shot #1040. The IFR output foil is 20 mils thick titanium. Peak beam current is 19 kA. Photo (c) is from shot #1042. The IFR output foil is 25 mils thick titanium. Peak current is 17 kA.

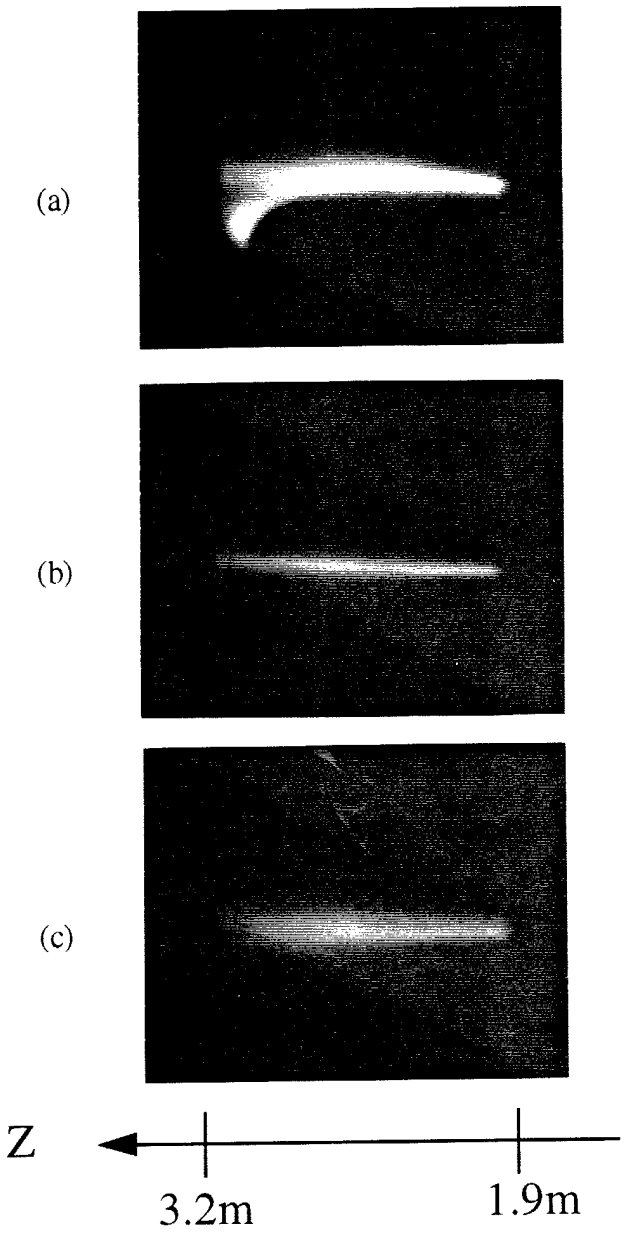

FIG. 6. Open-shutter photographs of three high current beams propagating in full density air. Conditioning is provided by an IFR cell followed by a B_θ cell as shown in Fig. 2. Photo (a) is from shot #2176. The wire current is I_{wire} = 3.9 kA. The beam current is I_{beam} = 15 kA. The output foil is 1.5 mils thick titanium. Again the e-beam is propagating from right to left in the photo. The photo shows the range between 1.9 m and 3.2 m downstream of the B_θ cell. Photo (b): shot #2177, I_{wire} = 4.3 kA, I_{beam} = 9 kA. Photo (c): shot #2174, I_{wire} = 6.3 kA, I_{beam} = 18 kA.

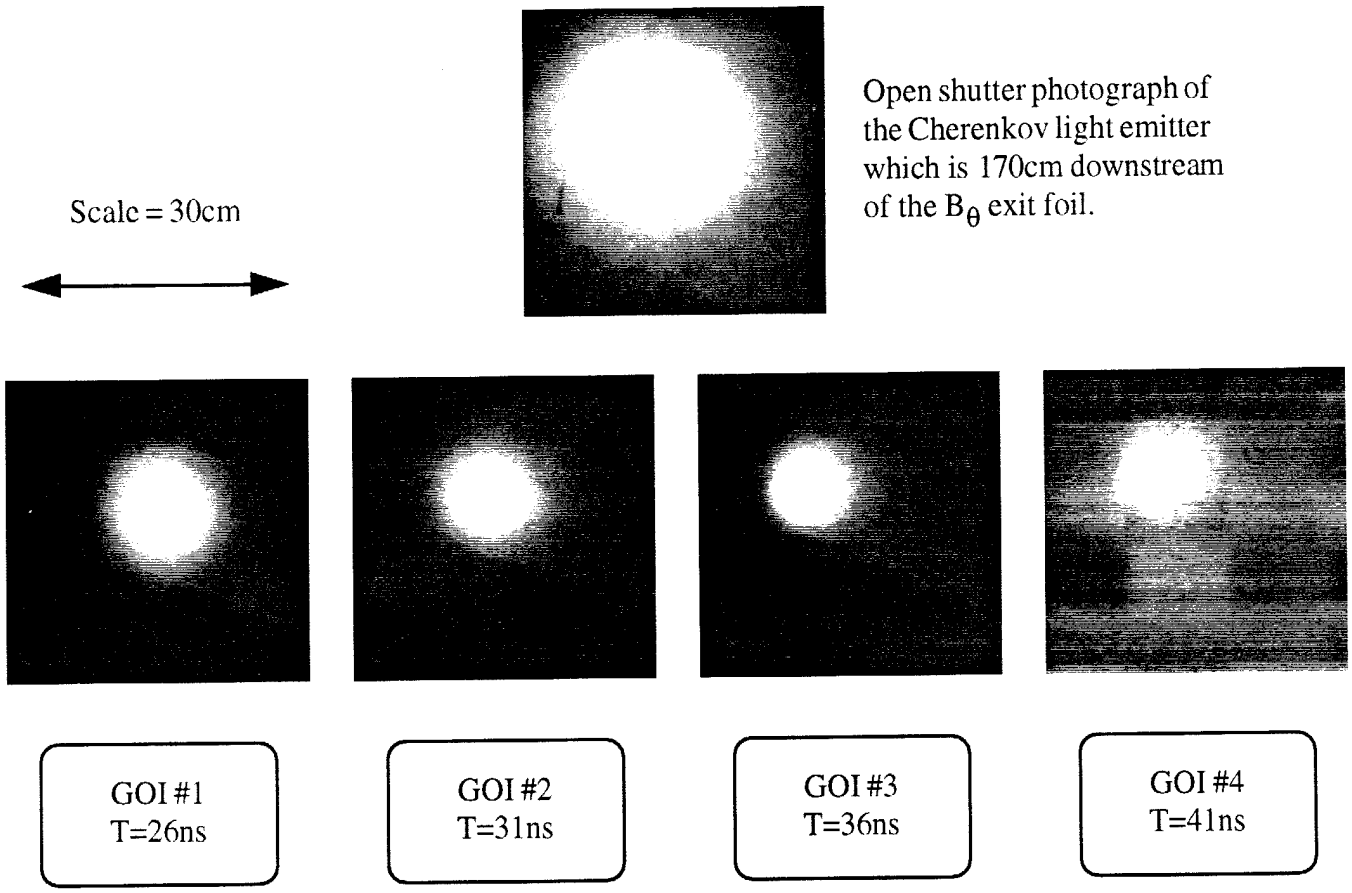

FIG. 7. Open shutter photograph and four frames from the GOI camera which illustrate a shot with low amplitude hose oscillations at Z=170 cm downstream of the B_θ cell exit foil.

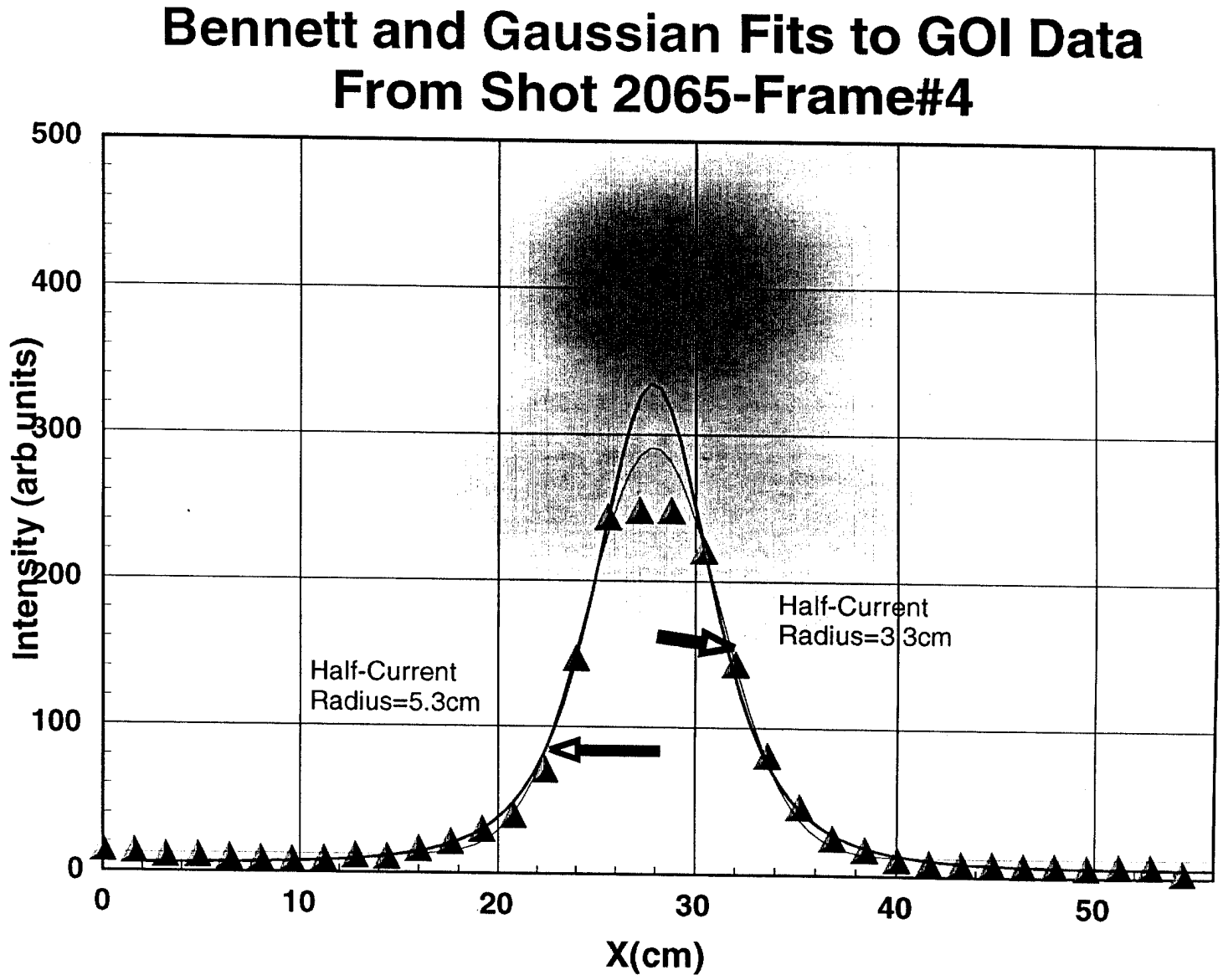

FIG. 8. An image from Shot 2065, GOI frame #4 with fitted Gaussian and Bennett profiles to the intensity data from a horizontal lineout through the center of the image.

(a)

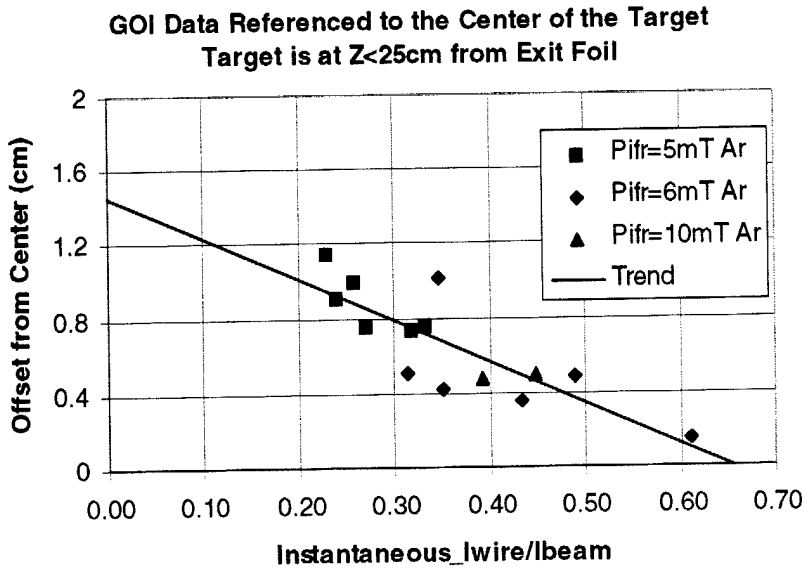

(b)

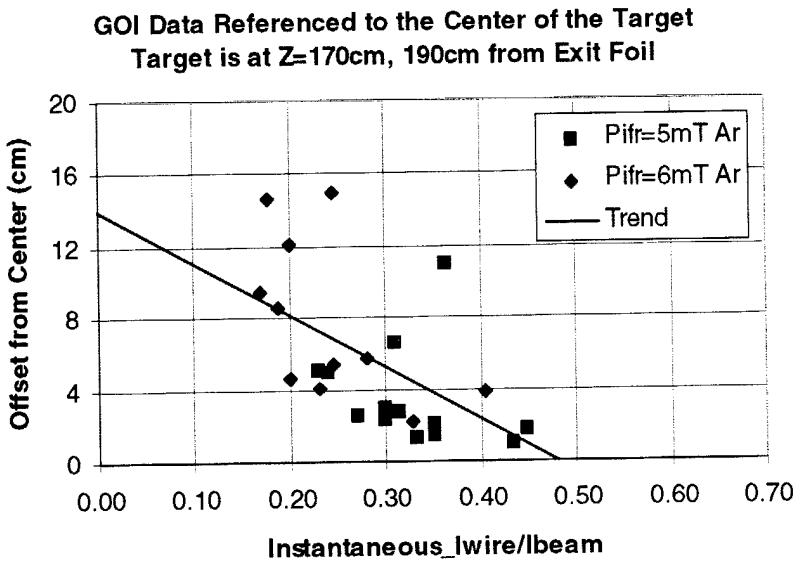

FIG. 9. Data from the GOI framing camera taken from images of the electron beam as it passed through a Cherenkov light emitter. In graph (a) the target was less than 25 cm from the B_θ exit foil. In graph (b) the target was at either 170 cm or 190 cm from the B_θ exit foil. The IFR cell gas was either 5, 6, or 10 mTorr of argon.. The distance from the center of the beam image to the center of the target is plotted on the vertical axis. The ratio of the wire current to the beam current at the time the image was taken is plotted on the horizontal axis.

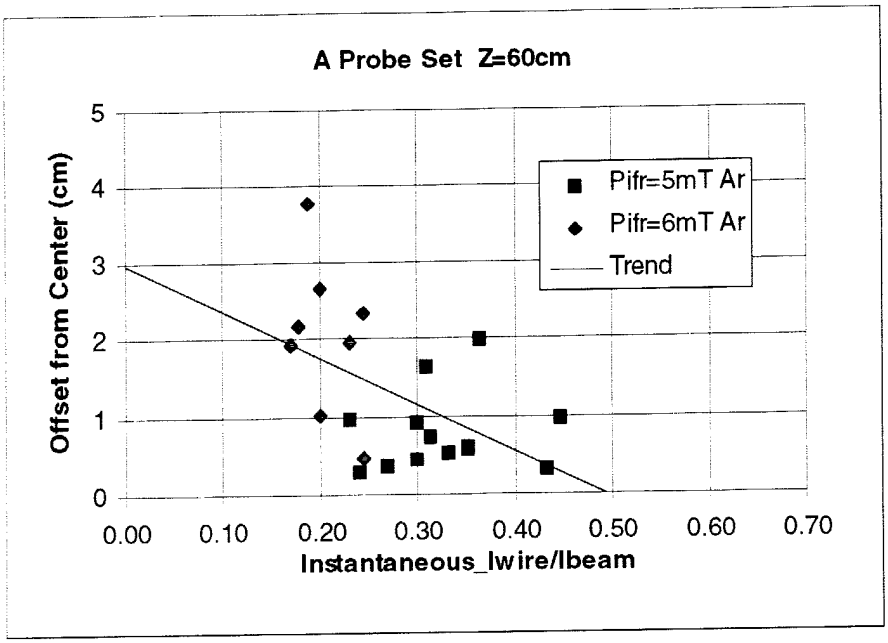

FIG. 10. Data from the 'A' magnetic probe set which was 60 cm downstream of the B_θ exit foil. The set consists of four magnetic field sensors which measure the net current centroid position as a function of time as the beam passes by. The data points were chosen at times simultaneous with GOI images of the beam. The IFR cell gas was either 5 or 6 mTorr of argon. There was only a small difference in the radius taper of the beam between the two IFR cell pressures. The distance from the center of the probe set to the centroid position of the net current is plotted on the vertical axis. The ratio of the wire current to the beam current at the time of the GOI image is plotted on the horizontal axis.